Journal of Science and Technology in Civil Engineering NUCE 2019. 13 (1): 1–11

AN EXPERIMENTAL STUDY ON FLEXURAL BEHAVIOR OF CORRODED REINFORCED CONCRETE BEAMS USING ELECTROCHEMICAL ACCELERATED CORROSION METHOD

Nguyen Ngoc Tan[a,*], Nguyen Dang Nguyen[a]

[a] *Faculty of Building and Industrial Construction, National University of Civil Engineering, 55 Giai Phong road, Hai Ba Trung district, Hanoi, Vietnam*

Article history:
Received 08 January 2019, Revised 16 January 2019, Accepted 17 January 2019

Abstract

This study investigated experimental bearing capacity of corroded reinforced concrete beams. Six testing beams were made of concrete having compressive strength of 25 MPa, with the dimensions of 80 × 120 × 1200 mm. They were divided into two groups depending of tension reinforcement ratio. Of which, two beams were used as the controls, whereas the other fours ones having tension reinforcement were subjected to corrosion by the electrochemical accelerated corrosion method. After accelerated corrosion, the beams were tested under monotonic loading to investigate their performance. All the tested beams were failed in flexural failure mode corresponding to spalling of cover concrete. Test results showed that as corrosion rate in tension reinforcement increased, the lower cracking load and the displacement at the cracking load were observed. As the corrosion rate of tension reinforcement ranging from 7.5% to 8.3%, it had little effect on the peak load. As the corrosion rate increased further, approximately 10.8% and 14.1% in this study, the peak load decreased significantly. The higher the corrosion rate, the lower the displacement of corroded beams. Moreover, as corrosion rate of tension reinforcement increased the number of concrete cracks and their spacing reduced, and the width of cracks was generally larger.

Keywords: reinforced concrete beam; electrochemical accelerated corrosion; corrosion rate; load-carrying capacity; displacement; concrete cracking.

https://doi.org/10.31814/stce.nuce2019-13(1)-01

1. Introduction

The reinforced concrete was used more than a century ago because it is a flexible, economic, and sustainable structure. In the process of exploitation and use of the work, reinforcement corrosion is one of the major cause which deteriorate behavior of RC structures. Corrosion attack can be classified into two sources which are carbonation of concrete or chloride penetration. The former typically induces uniform corrosion, whereas the latter causes non-uniform corrosion refers to as pitting corrosion. Uniform corrosion can be evaluated simply by reducing cross-sectional area and using the corresponding properties for uncorroded bar [1, 2]. Meanwhile, pitting corrosion localizing stress at pitting locations reduces strength and ductility of the reinforcing steel [1–4]. Furthermore, expansion of corrosion products, which is about 2-6 times the volume of virgin steel [5], exerts tensile stress to the surrounding concrete and ultimately causing cracking even spalling of cover concrete [6, 7]. In

*Corresponding author. *E-mail address:* tannn@nuce.edu.vn (Tan, N. N.)

addition, the corrosion of steel bars can also cause weakening of the bond and anchorage between concrete and reinforcement [8–11]. Consequently, the stiffness, strength and deformation capacities of RC members are reduced and the safety and serviceability of the structure are impaired [12–15].

In fact, two main causes of corrosion in reinforced concrete structures are: (i) Carbonation of concrete due to the infiltration of CO_2; (ii) attack of chloride ions [16, 17]. In the first case, the carbon dioxide in the air penetrates the cover concrete through a network of voids and cracks. With the presence of a liquid phase in concrete and hydrocarbon products of cement, especially $Ca(OH)_2$, the carbonation reaction occurs to form $CaCO_3$ (limestone). The pH of the cementitious media is decreased from about 12.5 to 13.5 to approximately 9.0, resulting in the disruption of the passive protective membrane to the reinforcement. In the second case, due to the liquid phase, chloride ions penetrate into the structure, change the condition of the concrete's protection environment to the reinforcement. This phenomenon results in morphological changes of the passive membrane, and thereby accelerating the corrosion process in the structure.

The data collected shows that the frequency and the cost of work repair for damage and degradation caused by corrosion has been increasing [17]. In Japan, a study indicated that 90% of existing RC structures have been exposed to the marine environment with protection concrete layer been not large enough and only 10-year-old works damaged are accounted for a large proportion. In the United States, based on the track of 586000 highway bridges, 15% of them have damaged structures, primarily due to aggressive corrosion. Vietnam has a very long coastline and major cities are not far away from the coastline. In our country, many coastal RC structures built from the 1960s to now have been applied building codes with little attention to the requirements for protection against corrosion under TCVN 9346:2012 [18]. In Vietnam, the effects of corrosion are more apparent than in other countries in the world, due to climatic conditions, temperatures, high humidity, large wet periods, high chloride ion concentration. Many works are severely affected by the corrosion process after a short time of use. Fig. 1 illustrates the severe corrosion situation of some existing RC structures in Vietnam [19].

(a) Corroded RC beam at a distance of 1 km from the coastline in Hai Phong province

(b) Corroded RC beam at a distance of 20 km from the coastline in Thanh Hoa province

Figure 1. Reinforcement corrosion in existing corroded structures [19]

Corrosion of steel reinforcement for sure is an important issue which has attracted more attention from the Vietnamese researchers recently [20, 21]. Local studies on corrosion problems and its effects have limited as the actual corrosion time is measured in units of year. This study was conducted to give an experimental procedure that allows for the creation of reinforced concrete structure in various corrosion levels in the laboratory for a reasonable time by using electrochemical accelerated corrosion method. Small-scale beam specimens are used. Beam specimens were tested under monotonic loading to investigate their behavior. This research is significant in that it advances the understanding of behavior of corroded reinforced concrete beams, which lays the foundation for further study on effect of reinforcement corrosion on reinforced concrete structures and assessing the durability of Vietnam maritime RC structures.

2. Experimental program

2.1. Materials used

The testing samples in this study were conducted at the Laboratory of Construction Testing and Inspection - National University of Civil Engineering. They were made of the concrete with B20 grade. Table 1 shows the aggregate component of concrete used. The compressive strength of concrete was determined by compression test on standard cubic samples with the dimensions of 150×150×150 mm in accordance with TCVN 3118:1993 [22]. The compressive strength of concrete was the average value of a sample group of three pellets. The axial compressive strength of concrete manufactured in 28-days is R_{28} = 25 MPa (see Table 1). The longitudinal reinforcements are the deformed bars with nominal diameters of 8 mm and 10 mm having the steel grade of CB300-V (under TCVN 1651-2:2008 [23]). Stirrup is a plain bar with nominal diameter of 6 mm having the steel grade of CB240-T. For each type of reinforcement diameter, a group of three steel bars was tested according to TCVN 197-1:2014 [24] to determine the actual tensile strength. The average results of tension test of the sample groups are shown in Table 2.

Table 1. Concrete mix and compressive strength at 28 days

Grade	Cement PCB40 (kg)	Sand (kg)	Gravel (kg)	Water (liter)	R28 (MPa)
B20	325	680	1240	195	25.0

Table 2. Mechanical properties of steel bars

Type of steel	Area (mm^2)	Yield strength f_y (MPa)	Ultimate strength f_u (MPa)	Ultimate strain ε_{su} (%)
D6 plain bar	28.3	288.6	419.3	29.3
D8 deformed bar	50.3	334.0	437.4	25.7
D10 deformed bar	78.5	337.3	437.4	23.7

2.2. Design of testing beams

There are six testing beams were divided into two groups that were cast with the details shown in Fig. 2. These beams were made has cross section of 80 × 120 mm (width × length); the concrete protective layer is 15 mm and the beam length is 1200 mm. There was 2D6 steel bars on the top side for hanging purpose. The rectangular stirrups No. 3 in the section 1-1 were D4a150 along 400 mm segment at two ends and D4a300 at the mid-span segment. The stirrup was plain bar. The difference between the two groups was the two longitudinal reinforcing bars at the bottom (No. 1), which were 2D8 deformed bars and 2D10 deformed bars for Groups 1 and 2, respectively.

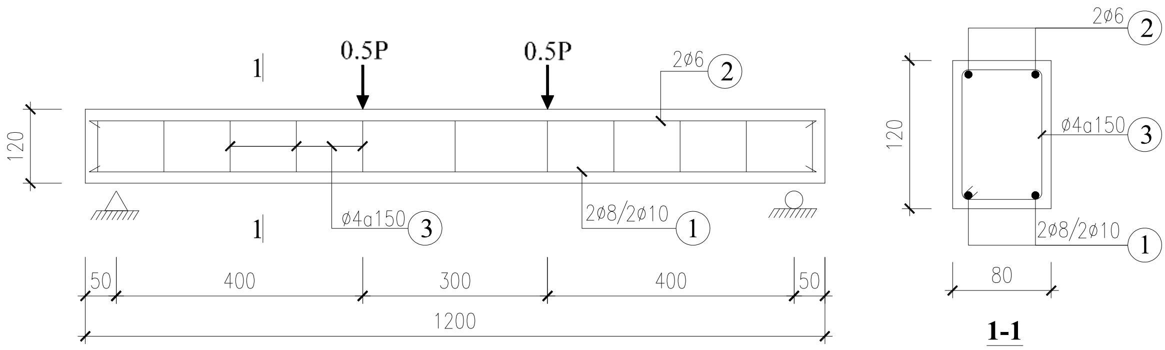

Figure 2. Dimensions of D8 and D10 testing beams

3. Electrochemical accelerated corrosion method

3.1. Diagram of corrosion experiments

After curing the experiment samples for at least 28 days, the reinforcement was induced corrosion by electrochemical accelerated corrosion methods. The two beam samples in each sample group are corroded, named D8-2, D8-3, D10-2, and D10-3. Two remaining beams (named D8-1 and D10-1) are not corroded and will be used as control beams. Fig. 3 illustrates the electrochemical accelerated corrosion method. The longitudinal rebars (D8 or D10) of the testing samples were connected to the anode of a DC power supply. The cathode of the DC supply power was connected to a copper bar placed in NaCl solution of 3.5% concentration (35g NaCl in 1 liter of water). With this NaCl content, salt water has the salinity equivalent to that of seawater in Vietnam and in the world, and in the experiment, it served as the electrolyte solution. The DC power supply allows converting alternating current into direct current. In this experiment, a voltage $U = 5$ V was maintained stability during the implementation of electrochemical corrosion. The maximum period of electrochemical corrosion testing was 14 days (336 hours) for D8-3 and D10-3 beams.

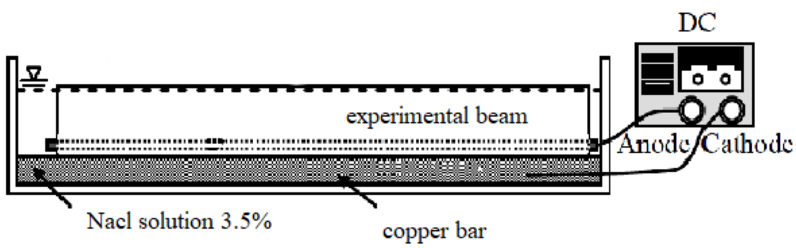

Figure 3. Accelerated corrosion setup

3.2. Testing setup and measuring instruments

After electrochemical accelerated corrosion of corroded beams and after curing for at least 28 days with non-corroded beams, the testing samples were subjected to monotonic loading to investigate their performance. In the test, the 1200 mm-length specimen was singly supported over a span of 1100 mm and was subjected to two symmetrical concentrated loads at points $P1$ and $P2$ which were both at a distance of 400 mm from the supports $R1$ and $R2$. The loads were generated by means of a hydraulic jack and an oil pump by hand. A load cell was used to measure the load applied during the test. Three Linear Variable Deformation Transducers (LVDTs) were installed to measure the vertical displacement of each tested beam. The sets of displacement transducers ($I1$ and $I3$) were used to measure the displacement at the supports ($R1$ and $R3$), respectively. The $I2$ displacement transducer was used to measure the displacement at mid-span of the beam. All displacement transducers were connected to a TDS-530 data-logger and a computer to collect automatically measurement data in order to establish the relationship between applied load and displacement. Fig. 4(a) shows the loading diagram and arrangement of the measuring instruments.

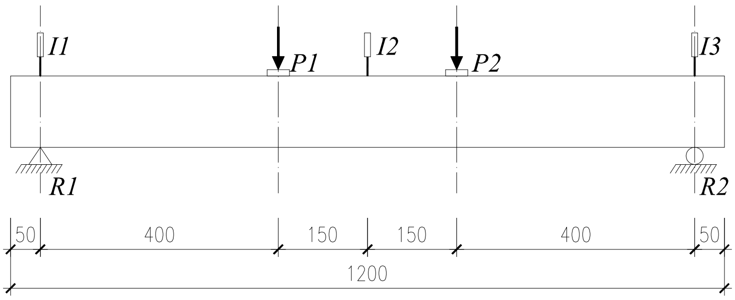

(a) Diagram of 4-point bending test

(b) Photo of testing beam

Figure 4. Loading experiment diagram

Fig. 4(b) shows a photo of the bending test on a typical beam. During the experiment, the applied load was continuously increased until the beam failed. At the same time, each testing beam was observed carefully to detect the appearance of the first concrete cracking. The development of concrete cracks was highlighted on the testing beam surface. After the end of the experiment, the distance between the concrete crackings was measured for the tested beams.

4. Experimental results and discussion

4.1. Corrosion rate of reinforcements

The reinforcement corrosion rate of beam tested was calculated based on the mass of the lost metal for the bearing principal bars. The steel bars were weighed to determine the mass before making the corrosion experiments (m_0). After the corroded beams were subjected to monotonic loading, they were demolished and the corroded reinforcement was extracted for corrosion measurement. The reinforcement was firstly cleaned by a bristle brush to remove concrete adhering to the surface. The reinforcement is then immersed in 5% HCl solution with 3.5 g hexamethylenetetramine for 1 day and then cleaned to remove corrosion products. The cleaning procedure was also applied to a control steel bar without corrosion. It was found the procedure resulted in insignificant loss of the steel of the control, uncorroded bar. Then, the bars were weighed to determine the remaining mass (m). The corrosion rate of the reinforcement, c (%) are defined by Eq. (1)

$$c\ (\%) = \frac{m_0 - m}{m_0} \times 100 = \frac{\Delta m}{m_0} \times 100 \tag{1}$$

where m_0 (g) being the stell mass before corrosion, m (g) being the stell mass after corrosion, and Δm (g) being the steel mass lost by corrosion.

Table 3 shows the results of the determination of reinforcement corrosion rate for all testing beams. For each corroded beam, the corrosion rate is the average value of the two corroded bars at the bottom layer (D8 or D10 steel bars).

Table 3. Determination of corrosion rates of D8 and D10 steel bars

No	Test group	Beam	m_0 (g)	m (g)	Δm (g)	c (%)	A_s (mm^2)
1		D8-1	390.0	-	-	-	50.30
2	Group 1	D8-2	390.0	360.8	29.3	7.5%	46.53
3		D8-3	390.0	348.0	42.3	10.8%	44.88
4		D10-1	554.5	-	-	-	78.50
5	Group 2	D10-2	554.5	508.5	46.0	8.3%	71.98
6		D10-3	554.5	476.0	78.5	14.1%	67.43

(a) Group 1 of D8 beams

(b) Group 1 of D10 beams

Figure 5. Overview of non-corroded beam and reinforcements corrosion rate of corroded beams

(a) Corroded steel bars in D8-2 beam with $c = 7.5\%$

(b) Corroded steel bars in D10-3 beam with $c = 14.1\%$

Figure 6. Close view on corroded steel bars

Fig. 5 shows the reinforcement photos after corrosion of the testing beams. It can be observed that all rebars are along the upper layer, the lower layer, and the stirrups were also corroded. The pitting corrosion was also observed for both the longitudinal bar and the stirrup. Especially, in the corners of the stirrup, it is shown at the degree of localized corrosion is higher (pitting corrosion) than at the other positions of the stirrup, as can be seen in Figs. 6(a) and 6(b). This was also observed in experiments on the corrosion made by [14, 15, 25]. Four corroded specimens did not display significant visible cracks. According to Uomoto and Misra [26] cases have been reported in which no visible cracks appear on the concrete surface despite severe corrosion of the reinforcement, especially when the diameter of the bars is less than 16 mm. In this study, maximum diameter of reinforcements has a diameter of only 10 mm, explaining why no visible cracks were found for D8-2, D8-3, D10-2, and D10-3 tested beams.

4.2. *Effect of reinforcement corrosion on the bearing capacity of the testing beams*

Figs. 7(a) and 7(b) show the response for testing groups of D8 and D10 beams, respectively. The control beams and corroded beams exhibited a typical flexural failure mode, as evidenced by the clear softening of hysteretic behavior before failure and no significant inclined cracks and/or fracture of stirrups were observed in the tests. The flexural cracks developed first on the bottom face of the specimen and propagated deep into the section as the displacement increased. When the concrete spalled, the flexural strength dropped drastically and hence the test was terminated.

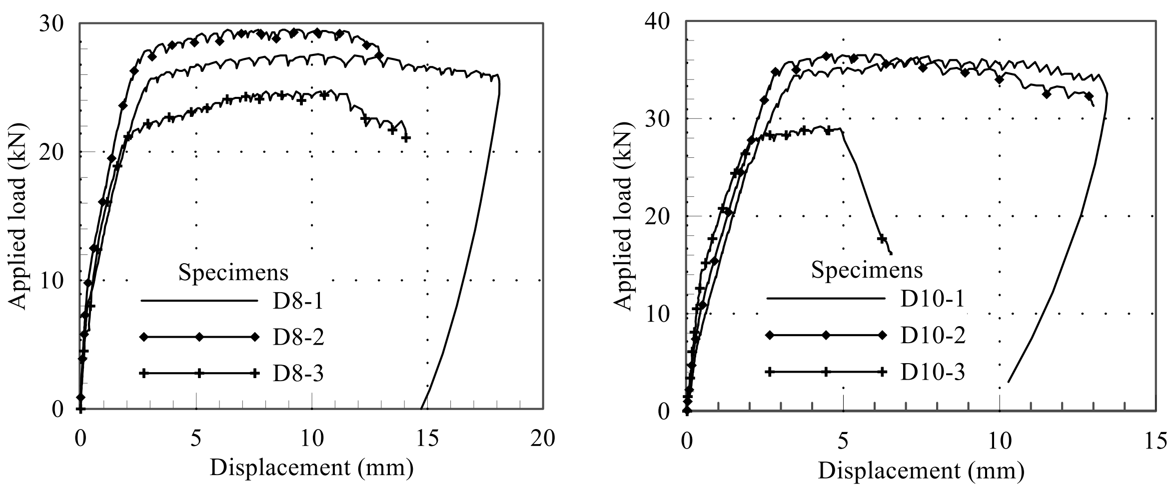

(a) Results of D8 beams

(b) Results of D10 beams

Figure 7. Load versus displacement for testing groups of D8 and D10 beams

The performance indicators include the cracking load (P_{cr}), cracking displacement (f_{cr}), and peak load (P_{peak}), ultimate displacement (f_u). The cracking load (P_{cr}) is considered as the applied load corresponding to the first concrete crack observed. The cracking displacement (f_{cr}) is the measured displacement at the cracking load. The peak load (P_{peak}) is the maximum applied load on each tested beam. The ultimate displacement (f_u) is defined as the displacement at the right time of terminating the test when the concrete spalled and the flexural strength dropped significantly. Table 4 summarizes the performance indicators for the beam specimens.

It can be observed that corroded beams in the two groups (D8-2 and D8-3 beams in Group 1; D10-2 and D10-3 beams in Group 2) showed similar phenomenon on the cracking load and the dis-

Table 4. Test results of D8 and D10 beam specimens

No	Test group	Beam	P_{cr} (kN)	f_{cr} (mm)	P_{peak} (kN)	f_u (mm)
1		D8-1	7.80	0.28	27.59	18.11
2	Group 1	D8-2	5.80	0.15	29.49	12.94
3		D8-3	5.30	0.15	24.79	14.07
4		D10-1	13.70	0.91	36.39	13.44
5	Group 2	D10-2	7.80	0.29	36.59	13.01
6		D10-3	6.30	0.18	29.19	6.60

placement at the cracking load. The higher the reinforcement corrosion rate, the lower the cracking load and the displacement at the cracking load. This is because corrosion induced expansion of the reinforcement, subsequently causing tensile stress in the cover concrete, and ultimately decreasing the cracking load.

Table 4 reveals that the peak load decreased when the reinforcement corrosion rate reach to a sufficient level. In this study, the percentage difference in the peak load of D8-2 corroded beam is compared to D8-1 non-corroded beam about 6.8% (29.49 versus 27.59 kN), and of D10-2 corroded beam is compared to D10-1 non-corroded beam about 0.5% (36.59 versus 36.39 kN), which are insignificant considering several factors such as material variation, size effect, and insufficient corrosion rates (about c = 7.5 – 8.3%) that could also produce such a difference amount. The peak load in the remaining tested beams (D8-3 and D10-3) significantly decreased with an increasing amount of reinforcement corrosion, about 10.1% to 19.8% in compared with the non-corroded beams. This can be explained by the reduction of cross-sectional area of tension steel bars due to sufficient corrosion rates (c = 10.8% for D8-3 beam, and c = 14.1% for D10-3 beam) and the reduction of the bond between steel bars and concrete.

The ultimate displacement of the tested beams decreased clearly when increasing the corrosion rates. For the D8 beams group, the displacement reduced approximately of 28.5% (f_u = 18.11 versus 12.94 mm) between the non-corroded and corroded beams. For the D10 beams group, this reduced approximately of 50.9% (f_u = 13.44 mm versus 6.60 mm) between the non-corroded and corroded beams. It is may be due to the fact that top reinforcements were also corroded, the expansion of corrosion product generated from top reinforcements induced tensile stress to the top cover concrete, which was consequently decreasing the compressive capacity of the concrete to balance the tensile force of the reinforcements. Thus, as corrosion rate increases the corroded beam may be failed earlier.

4.3. Effect of reinforcement corrosion on concrete cracking distribution

At the end of bending test, the length and spacing among the concrete cracks were measured and highlighted in Figs. 8 and 9. It is found that the number of concrete cracks on the non-corroded beams is more than that of corroded beams. Furthermore, crack spacings on the non-corroded beams are smaller than that of corroded beams, and the width of cracks on the corroded beams are generally larger than that of non-corroded beams. That is because reduction of bond reduces the ability of the section to mobilize the strain in the steel bars. The section must rotate more to yield the longitudinal reinforcement. Concrete capability to share tension from reinforcement (tension stiffening) is decreased due to bond reduction, subsequently decreasing the number of crack appeared in the beam and enlarging the width of the crack on the corroded beams.

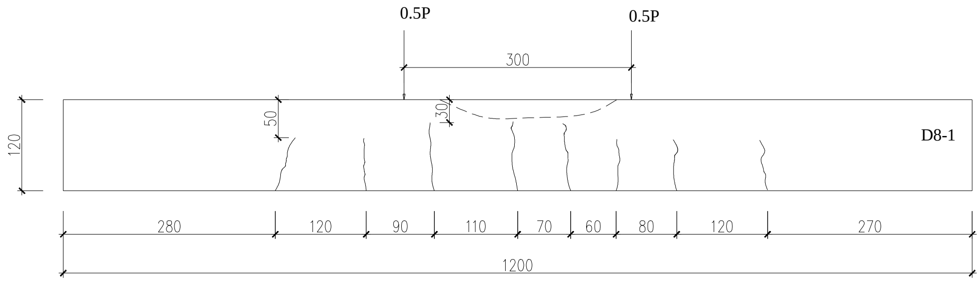

(a) Cracks distribution on the D8-1 beam

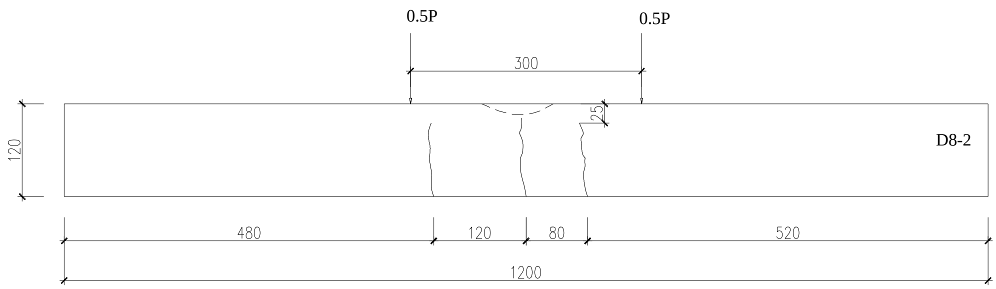

(b) Cracks distribution on the D8-2 beam

Figure 8. Comparison of the distribution of concrete cracks on D8 testing beams

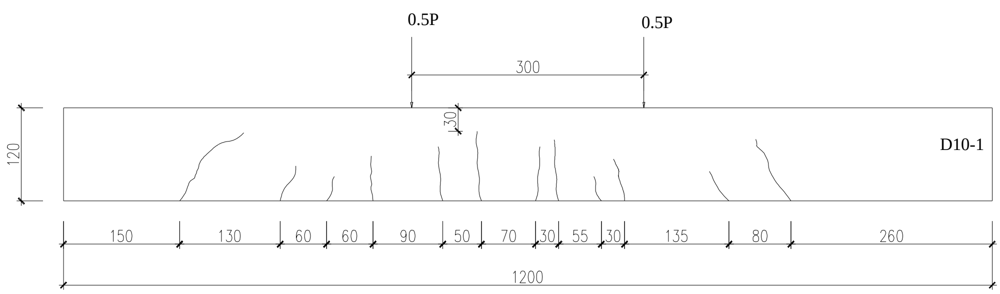

(a) Cracks distribution on the D10-1 beam

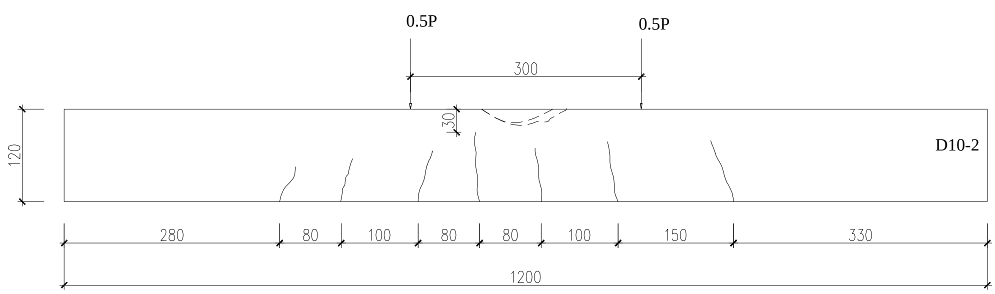

(b) Cracks distribution on the D10-2 beam

Figure 9. Comparison of the distribution of cracks on D10 testing beams

5. Conclusions

In this study, six reinforced concrete beams were fabricated and corrosion was induced to steel bars using the electrochemical accelerated corrosion method. The tested beams were subjected to four-point bending under monotonic loading to investigate their flexural behavior. Some main conclusions can be drawn as follows:

- Corrosion of transverse and longitudinal reinforcements was non-uniform. Larger corrosion pit depths were observed, particularly at the corners of the transverse steel hoops.

- The higher the reinforcement corrosion rate, the lower the cracking load and the displacement at the cracking load.

- As corrosion rate of tension reinforcement ranges from 7.5% to 8.3%, the peak load had not much apprarently difference with those of the non-corroded beams. As the corrosion rate being greater (about 10.8% to 14.1% in this study), the peak load of these tested beams significantly decreased about 10.1% to 19.8% in compared with that of the non-corroded beams.

- As corrosion rate increased the ultimate displacement of the corroded beams considerably decreased.

- The number of concrete cracks on the non-corroded beams was more than that of corroded beams. Furthermore, the higher the corrosion rates, the smaller of cracks spacing and generally the larger of crack width.

References

[1] Du, Y. G., Clark, L. A., Chan, A. H. C. (2005). Effect of corrosion on ductility of reinforcing bars. *Magazine of Concrete Research*, 57(7):407–419.

[2] Du, Y. G., Clark, L. A., Chan, A. H. C. (2005). Residual capacity of corroded reinforcing bars. *Magazine of Concrete Research*, 57(3):135–147.

[3] Kashani, M. M., Crewe, A. J., Alexander, N. A. (2013). Nonlinear stress–strain behaviour of corrosion-damaged reinforcing bars including inelastic buckling. *Engineering Structures*, 48:417–429.

[4] Kashani, M. M., Crewe, A. J., Alexander, N. A. (2013). Use of a 3D optical measurement technique for stochastic corrosion pattern analysis of reinforcing bars subjected to accelerated corrosion. *Corrosion Science*, 73:208–221.

[5] Liu, Y., Weyers, R. E. (1998). Modeling time-to-corrosion cracking in chloride contaminated reinforced concrete structures. *ACI Materials Journal*, 96(6):675–681.

[6] Williamson, S. J., Clark, L. A. (2000). Pressure required to cause cover cracking of concrete due to reinforcement corrosion. *Magazine of Concrete Research*, 52(6):455–467.

[7] Andrade, C., Alonso, C., Molina, F. (1993). Cover cracking as a function of bar corrosion: Part I-Experimental test. *Materials and Structures*, 26(8):453–464.

[8] Al-Sulaimani, G. J., Kaleemullah, M., Basunbul, I. A., Rasheeduzzafar (1990). Influence of corrosion and cracking on bond behavior and strength of reinforced concrete members. *ACI Structural Journal*, 87 (2):220–230.

[9] Amleh, L., Mirza, S. (1999). Corrosion influence on bond between steel and concrete. *ACI Structural Journal*, 96(3):415–423.

[10] Azad, A. K., Ahmad, S., Azher, S. A. (2007). Residual strength of corrosion-damaged reinforced concrete beams. *ACI Materials Journal*, 104(1):40–47.

[11] Mangat, P. S., Elgarf, M. S. (1999). Flexural strength of concrete beams with corroding reinforcement. *ACI Structural Journal*, 96(1):149–158.

[12] Rodriguez, J., Ortega, L. M., Casal, J. (1997). Load carrying capacity of concrete structures with corroded reinforcement. *Construction and Building Materials*, 11(4):239–248.

[13] Torres-Acosta, A. A., Navarro-Gutierrez, S., Terán-Guillén, J. (2007). Residual flexure capacity of corroded reinforced concrete beams. *Engineering Structures*, 29(6):1145–1152.

[14] Ou, Y.-C., Tsai, L.-L., Chen, H.-H. (2012). Cyclic performance of large-scale corroded reinforced concrete beams. *Earthquake Engineering & Structural Dynamics*, 41(4):593–604.

[15] Ou, Y.-C., Nguyen, N. D. (2016). Influences of location of reinforcement corrosion on seismic performance of corroded reinforced concrete beams. *Engineering Structures*, 126:210–223.

[16] Broomfield, J. P. (2003). *Corrosion of steel in concrete: understanding, investigation and repair*. Taylor & Francis, New York, USA.

[17] Ollivier, J. P., Vichot, A. (2008). *La durabilité des bétons: bases scientifiques pour la formulation de bétons durables dans leur environnement*. Presses des Ponts, 844 p.

[18] TCVN 9346:2012. *Concrete and reinforced concrete structures - Requirementd of protection from corrosion in marine environment*. (in Vietnamsese).

[19] Ministry of Construction (2016). *Training and experimental training of concrete and reinforced concrete corrosion material*. (in Vietnamsese).

[20] Nguyen, N. T. (2018). *Study on establishing the acclerated testing of steel bar in reinforced concrete for assessing the durability of marine structures*. Project number 150-2017/KHXD-TD. National University of Civil Engineering.

[21] Nguyen, N. T., Tran, A. D., Nguyen, C. T., Trinh, B. T., Luong, T. A. (2018). An experimental study to identify the influence of reinforcement corrosion on concrete-steel bond stress. *Journal of Science and Technology in Civil Engineering*, 12(6):29–38. (in Vietnamsese).

[22] TCVN 3118:1993. *Heavyweight concrete - Method for determination of compressive strength*. (in Vietnamsese).

[23] TCVN 1651-2:2008. *Steel for the reinforcement of concrete – Part 2: Ribbed bar*. (in Vietnamsese).

[24] TCVN 197-1:2014. *Metallic materials - Tensile testing - Part 1: Method of test at room temperature*. (in Vietnamsese).

[25] Higgins, C., Farrow III, W. C. (2006). Tests of reinforced concrete beams with corrosion-damaged stirrups. *ACI Structural Journal*, 103(1):133–141.

[26] Uomoto, T., Misra, S. (1988). Behavior of concrete beams and columns in marine environment when corrosion of reinforcing bars takes place. *ACI Special Publication*, 109:127–146.